

TRANSITION TO A GAPLESS PEIERLS INSULATOR IN HEAVILY-DOPED POLYACETYLENE

X.Q. Yang* and D.B. Tanner

Department of Physics, University of Florida, Gainesville, FL 32611, USA

and

M.J. Rice, H.W. Gibson,[†] A. Feldblum[‡] and A.J. Epstein[§]

Xerox Webster Research Center, Webster, NY 14580, USA

(Received 24 March 1986; in revised form 1 September 1986 by R.H. Silsbee)

At high doping concentrations, polyacetylene undergoes a transformation into a state characterized by high d.c. conductivity, by a large Pauli susceptibility and by the absence of the interband transition of the undoped polymer. The optical spectrum shows a pseudogap at ≈ 0.2 eV and vibrational modes which imply that the carbon–carbon bond length is not uniform. We conclude that this state is best described as a gapless incommensurate Peierls insulator.

1. INTRODUCTION

BEGINNING WITH THE earliest studies, the electronic properties of heavily doped *trans*-(CH)_x have been described as “metallic”. The metallic state is thought to occur because the bond alternation of the undoped polymer is suppressed by doping, leading to closure of the semiconducting energy gap. This picture has been used to describe the results of transport [1–3], magnetic susceptibility [3–6], specific heat [7], far-infrared [1], optical [8] and electron energy-loss [9] studies. In this paper we show that the magnetic, optical, and transport properties of [CH(CIO₄)_y]_x with $y > 0.04$ are not metallic but instead are best described as those of a one-dimensional system stabilized by an incommensurate charge-density wave distortion [10]. On account of the strong disorder in the material and the consequent short relaxation time for the charge carriers, the usual Peierls gap is replaced by a pseudogap so that a large density-of-states exists at the Fermi level [11, 12]. Such a state

for polyacetylene has been theoretically predicted by Mele and Rice [13]. The onset of this gapless Peierls state is heralded by a rapid rise of the Pauli contribution to the spin susceptibility and by the disappearance of the $2\Delta_c = 1.4$ eV interband transition in the optical absorption spectrum. The conductivity is high ($\sigma_{RT} > 100 \Omega^{-1} \text{cm}^{-1}$) and depends weakly on temperature and concentration; the thermopower is small ($S_{RT} = 10 \mu\text{V K}^{-1}$) and varies linearly with temperature.

2. EXPERIMENTAL DETAILS

Polyacetylene, produced by the Shirakawa technique [14], was doped electrochemically with ClO₄[−] ions from a solution of LiClO₄ in acetonitrile using Pt as a counter electrode. Concentrations were determined by weight uptake. Each doped film was cut up and portions were distributed for the measurements. The magnetic susceptibility was measured with a high-field Faraday balance. Four-probe electrical conductivity and thermopower measurements were done simultaneously in a closed-cycle refrigerator. Reflectance measurements were done with a Michelson interferometer in the far infrared and a grating monochromator in the infrared and visible; the frequency-dependent conductivity $\sigma_1(\omega)$ was determined by Kramers–Kronig analysis. We used the shiny side of the films for our measurements to minimize diffuse reflectance, although it is possible that the fibrillar morphology of the samples affected the results. In this paper we have drawn most of our conclusions from a comparison of $\sigma_1(\omega)$ in three different doping regions; the basic morphology is similar in all samples.

*Present Address: Division of Material Science, Bldg. 480, Brookhaven National Lab., Upton, NY 11973, USA.

[†]Present Address: Signal UOP Research Center, 50 UOP Plaza, Des Plaines, IL 60016, USA.

[‡]Present Address: AT & T Technologies, Engineering Research Center, P.O. Box 900, Princeton, NJ 08540, USA.

[§]Present Address: Department of Physics and Department of Chemistry, Ohio State University, Columbus OH 43210, USA.

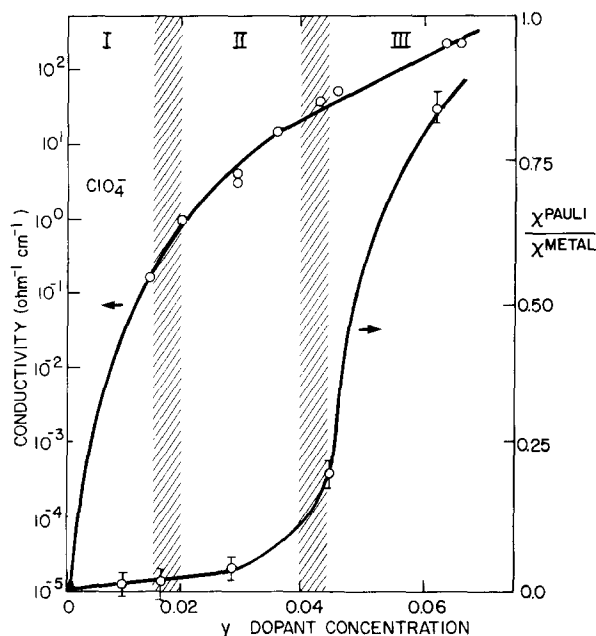


Fig. 1. Room-temperature dc conductivity and magnetic susceptibility of $[\text{CH}(\text{ClO}_4)_y]_x$ vs dopant concentration. Lines are guides to the eye.

3. MAGNETIC AND TRANSPORT RESULTS

The effect of doping on the room-temperature conductivity σ_{RT} and on the Pauli susceptibility χ^{PAULI} is shown in Fig. 1. χ^{PAULI} is directly proportional to the Fermi-energy density-of-states, $N(E_F)$. The susceptibility has been normalized by $\chi^{\text{METAL}} = \mu_B^2 N_0$, where χ^{METAL} is the susceptibility of "metallic" $(\text{CH})_x$ in the absence of Coulomb repulsion and N_0 is the expected value of $N(E_F)$ for "metallic" polyacetylene. We estimated N_0 by assuming a half-filled, one-dimensional, tight-binding band of width $W = 10 \text{ eV}$, for which $N_0 = 4/W\pi = 0.13 \text{ states/(eV} - C_{\text{atom}})$. Three regions may be identified in these data. Region I, with $0 \leq y < 0.02$, has low values of both σ_{RT} and $N(E_F)$. The electronic structure in this light doping regime is that of semiconducting $(\text{CH})_x$ with relatively isolated charged solitons [15] induced by doping, although band tailing due to disorder is important [16]. In region II, where $0.02 < y < 0.04$, the conductivity is quite high yet $N(E_F)$ is low. An even lower $N(E_F)$ has recently been observed in Na doped samples [5]. Our previous studies [16] of I_3 -doped samples in region II have established that each dopant molecule produces a charged soliton with transport occurring via variable-range hopping among soliton-like states near E_F . A similar analysis using an energy-dependent $N(E)$ has been applied to our regions I and II ClO_4 -doped samples [16]. Region III, with $0.04 < y < 0.08$ is the principal subject of this study. Here, both

σ_{RT} and $N(E_F)$ are high, although $N(E_F)$ reaches only about 80% of the value expected for metallic $(\text{CH})_x$. Reduced values for $N(E_F)$ in this region have been observed [4, 5] in I_3 , AsF_5 , and Na doped $(\text{CH})_x$.

The temperature-dependence of the conductivity of region III samples differs from that at lower doping concentrations. In the latter case [16], $\sigma \sim \exp[-(T_0/T)^\alpha]$ with $\alpha = 1/4$ for a constant density-of-states near E_F and $\alpha = 1/2$ for a quadratic variation around E_F , in accord with variable-range hopping transport [16]. Region III samples cannot be made to fit this equation with realistic parameters for any value of α . Instead, we observe a simple power law behavior of the conductivity, $\sigma \sim T^{0.6}$, between 30 and 300 K. This temperature dependence is neither that of a metal (where σ decreases with increasing T) nor that of a disordered insulator.

We note that there exists also a fourth region, $y > 0.08$. Our samples at these doping levels show clear signs of degradation: whereas some portions behave as do samples in region III, other have very low conductivity, are black in color, show a re-emergence of the semiconducting interband transition, and are extremely brittle.

4. OPTICAL PROPERTIES

Figure 2 shows the frequency-dependent conductivity of a sample in each region, with region I represented by $y = 0.016$, region II by $y = 0.034$, and region III by $y = 0.061$. The optical transition between the valence band and conduction band of the undoped polymer, which occurs [8] at $2\Delta_c = 11000 \text{ cm}^{-1}$ (1.4 eV), is seen as the dominant feature in region I. It is weaker in region II. And, it is essentially not observed in region III. This transition is absent in all of our samples with $y \geq 0.045$. The doping-related midgap

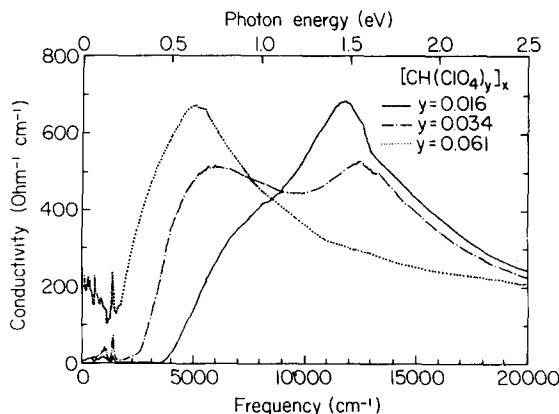


Fig. 2. Frequency-dependent conductivity of three samples of doped $(\text{CH})_x$.

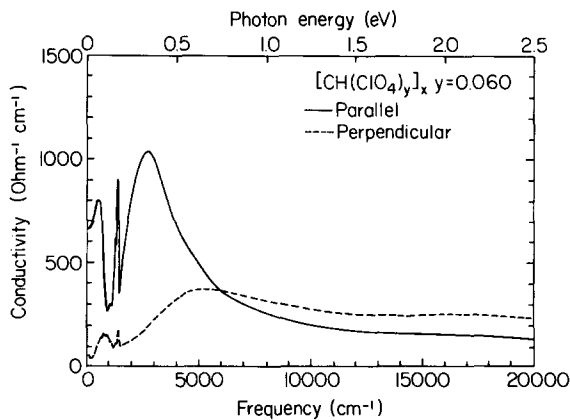


Fig. 3. Frequency-dependent conductivity of stretch-oriented, heavily-doped $(\text{CH})_x$.

absorption [17, 8], is a shoulder at 6000 cm^{-1} (0.75 eV) in region I samples. In region II, the strength of this absorption increases and the center frequency is lower. Finally, in region III, there is a peak at $4000\text{--}5000\text{ cm}^{-1}$ ($0.5\text{--}0.6\text{ eV}$), which is the only strong electronic absorption in the entire frequency region below 25000 cm^{-1} (3 eV).

Figure 3 shows $\sigma_1(\omega)$ of a partially oriented region III sample, prepared by stretching a piece of undoped $(\text{CH})_x$ to approximately 1.8 times its original length and then doping it. The interband transition at $2\Delta_c = 1.4\text{ eV}$ is observed in neither polarization. Instead, there is a single peak, which is seen to be much stronger for polarization along the polymer chain (i.e., the stretching direction), with an onset at $\approx 1500\text{ cm}^{-1}$ (0.2 eV) and a maximum at 3000 cm^{-1} (0.4 eV). Note that this peak is at a substantially lower energy than the “midgap” absorption, which occurs at 6000 cm^{-1} (0.7 eV) in region I samples.

The low frequency vibrational modes are also stronger for chain-axis polarization. In region I and II samples, narrow lines [18] at 1290 cm^{-1} and 1400 cm^{-1} were initially associated with internal vibrations of the charged soliton [19]. More recently it has been shown [20, 21] that any charged defect which breaks the bond alternation will lead to doping-induced infrared active localized phonons near Raman-active mode frequencies. The infrared absorption could result from solitons, polarons, or bipolarons. (Note that polaron — but not soliton or bipolaron — defects are ruled out by the absence of doping-induced magnetic susceptibility in regions I and II). The broad maximum occurring between 500 and 900 cm^{-1} is thought to be the “pinning” mode of the soliton [20]. These features are present in all three regimes with an oscillator strength proportional to dopant concentration [10].

That region III samples have these vibrational features in their spectra [10, 22] is evidence against the picture of heavily-doped $(\text{CH})_x$ as a simple metal. If the bond lengths were uniform and the gap closed, then these vibrations presumably would be infrared inactive.

5. POLYACETYLENE AS A GAPLESS PEIERLS INSULATOR

To reconcile the evidence for non-uniform bond lengths and gap with the high conductivity and susceptibility of Fig. 1 and the absence of the interband transition at 1.4 eV in the data of Figs. 2 and 3, we propose that heavily-doped polyacetylene is best described as a gapless incommensurate Peierls insulator. In the absence of disorder and as a function of increasing charge added to (or removed from) the half-filled band, the Peierls distortion evolves continuously from a mostly commensurate phase, in which the added charge is stored in soliton or local discommensuration centers, to a phase that is incommensurate throughout and in which the added charge is uniformly delocalized. Although the system formally is always incommensurate, we shall refer to the two limits of qualitatively differing behavior as “commensurate” and “incommensurate” respectively. According to this model, the one-dimensional instability, which is responsible for bond alternation in the undoped polymer, still is dominant at high doping levels but the distortion is incommensurate with the lattice. The Peierls distortion ordinarily would render the polymer an insulator but on account of the known [23] strong disorder the gapless state exists with finite Fermi-surface density of states and d.c. conductivity [11–13].

The model follows from the strong analogy between the Peierls insulator and BCS superconductor. Impurity scattering has the same pair-breaking effect on the Peierls insulator as magnetic impurity scattering in the superconductor. As shown by Schuster [11] and by Rice *et al.* [12], sufficiently strong impurity scattering induces in the Peierls insulator a gapless state, analogous to gapless superconductivity [24]. This behavior is also seen in the calculations of Mele and Rice [13].

This model makes several predictions. These are discussed and compared to experiment in the following paragraphs.

(a) Susceptibility

The density-of-states in the region of the Fermi energy is [12]

$$N(E) = N_0 [g + 1.5(E - E_F)^2 / \eta^2 \Delta^2 g^5], \quad (1)$$

where $\eta = (\hbar / \tau \Delta)$ is Peierls pair-breaking parameter, Δ is the usual incommensurate order parameter, τ is a mean electronic impurity scattering time and $g = (1 - \eta^{-2})^{1/2}$ measures the reduction in the Fermi-level

density-of-states, relative to N_0 , the metallic value. Experimentally, our region III samples have a susceptibility which is high but less than the "metallic" value (Fig. 1). The reduction of $N(E_F)$ to approximately 0.8 of the metallic value would imply $\eta \approx 1.67$.

(b) Optical absorption

When $\eta > 1$, Δ , or equivalent the amplitude of the incommensurate lattice distortion, $u = \Delta/2\gamma \sin(k_F a)$, is given by [12]

$$u = [\Delta_0/2\gamma \sin(k_F a)] \exp(-\phi(\eta)), \quad (2)$$

in which Δ_0 denotes the incommensurate order parameter in the absence of disorder scattering ($\tau^{-1} \rightarrow 0$), $\gamma = -\partial t/\partial a$ ($\approx 8 \text{ eV \AA}^{-1}$) is the derivative of the π -electron hopping integral with respect to interatomic separation, and $\phi(\eta) = \text{arccosh}(\eta) + (1/2) [\eta \arcsin(\eta^{-1}) - g]$. This incommensurate distortion permits anomalous IR activity of Raman active vibrational modes (phase phonons) [25]. The phase phonon absorption occurs at very near the same frequencies as the soliton (or other localized charged defect) internal vibrations and pinning mode. The theories of the phase phonon [25] and soliton vibrational absorption [19, 20] give expressions for the conductivity which are formally very similar for frequencies lower than the energy gap. In our measurements, region III samples have strong infrared absorption (Figs. 2 and 3) at 1290 and 1400 cm^{-1} . These frequencies are unchanged from the doping-induced absorption of the lightly-doped polymer.

The optical spectrum (Fig. 2) of the commensurate, soliton-containing phase (regions I and II) has two electronic excitations, the primary one at $2\Delta_c = 1.4 \text{ eV}$ and a second to midgap soliton levels. The optical spectrum of the gapless, incommensurate state (region III) has only a single excitation, from the valence band to a "condensate" band occupying the energy region where the soliton band previously existed. The disappearance of the primary interband transition is evidence that region III $(\text{CH})_x$ has entered the gapless incommensurate Peierls state. The movement to lower energies of a considerable density of one electron levels occasioned by the appearance of the pseudogap at E_F strongly suppressed the 1.4 eV interband transition oscillator strength. Calculations by Jestin *et al.* [26] and by Jeyadev and Conwell [27] suggest that the primary 1.4 eV interband excitation is absent in the incommensurate case because, not being a direct vertical excitation (in an extended zone scheme) it is not allowed by symmetry considerations.

(c) Conductivity

The d.c. conductivity is reduced from the Drude metallic value σ_0 according to [24, 28]

$$\sigma = \sigma_0 g^2. \quad (3)$$

Note that for $1 < \eta < \sqrt{3}$, the conductivity increases with increasing impurity scattering. We speculate that if phonon scattering contributed to the Peierls-pair-breaking parameter as does impurity scattering, an increase in temperature, which increases phonon scattering, could lead to an increase in conductivity.

In our region III samples, the d.c. and far-infrared conductivity are reduced to $\sigma_{\text{RT}} = 150 \Omega^{-1} \text{ cm}^{-1}$ from the Drude metallic value — which we interpret as approximately corresponding to the peak in $\sigma_1(\omega)$. Thus, $\sigma_0 = 700 \Omega^{-1} \text{ cm}^{-1}$. Although qualitatively in accord with our model, this reduction is much more than that quantitatively predicted by equation (3) with $\eta = 1.67$. The temperature dependence is in accord with the above speculation, increasing with increasing T .

Mele and Rice [13] find for the incommensurate isolated chain, $\Delta_0 = 0.25 \text{ eV}$. With $\eta = 1.67$, equation (2) yields $\Delta \approx 0.1 \text{ eV}$ so that $\tau = (\hbar/\eta\Delta) = 4 \times 10^{-15} \text{ sec}$. ($\hbar/\tau \approx 0.17 \text{ eV}$). Then (assuming a Fermi velocity of 10^8 cm sec^{-1}) the mean free path is $l \approx 40 \text{ \AA}$, in agreement with the structural coherence length [23]. In contrast, if simple metallic behavior is assumed, the effective d.c. conductivity would be $\sigma_{\text{RT}} = ne^2\tau/3m$ where $m \approx m_e$ is the effective mass of the conduction electrons, $n = 1.7 \times 10^{22} \text{ cm}^{-3}$ is their density, and the factor of 3 comes from an orientational average of fibril directions. The measured conductivity of $150 \Omega^{-1} \text{ cm}^{-1}$ then gives $\tau = 1 \times 10^{-16} \text{ sec}$ or $l \approx 1 \text{ \AA}$, shorter than the 1.4 \AA C—C spacing.

(d) Specific heat

The electronic specific heat of the gapless Peierls insulator possesses both a term linear in T and one which varies at T^3 . The latter should be an unusually large correction because according to equation (1) it will be of order $(T/T_F)(T/T_s)^2$ rather than $(T/T_F)^3$, where $k_B T_s = \Delta\eta g^{5/2} \ll k_B T_F$. Measurements by Moses *et al.* [7] show that the coefficient of the T^3 term in the specific heat increases by a factor of 6 upon heavy AsF_5 doping.

Thus despite the complexities of actual $(\text{CH})_x$ samples and our omission of Coulomb correlation effects [29], this model describes region III reasonably well.

We note that the rapidity of the "transition" to the gapless state as a function of concentration may be understood in terms of the relative suddenness of the onset of severe disordering of the CDW as its charge begins significantly to delocalize from soliton centers. This onset occurs approximately at concentrations for which soliton overlap begins, or more quantitatively [13], at the concentration $c^* = (E_s/W)$, or $c^* \approx 0.045$ for a bandwidth $W = 10 \text{ eV}$ and a soliton energy

$E_g \approx 0.45$ eV. The point is that the dopant ions cannot significantly disorder the Peierls system until the charge donated to it or removed from it (by the dopants) has delocalized; as soon as delocalization occurs the disorder is severe. For $y \ll c^*$ the only "disorder" is the displacement of soliton centers along the chains to positions that are adjacent to ionic dopants, a disorder that leaves the commensurate chain segments intact.

6. DISCUSSION

An early model [3] for polyacetylene was of strongly inhomogeneous doping, in which the equilibrium phases were assumed to be the undoped semiconducting polymer and a heavily doped, metallic phase. At intermediate doping levels, the sample would be a mixture of these two phases. The insulator to conductor transition was viewed as a percolation effect, occurring as the metallic volume fraction increased. Our data are not consistent with this two-phase picture. The presence of the doping-induced vibrational modes is inconsistent with the heavily-doped phase being a simple metal. In addition, although the simultaneous decrease of the interband transition and increase of the "midgap" transition would occur if the phases were small bandgap and large bandgap semiconductors, the sudden turn-on of the susceptibility (Fig. 1) cannot occur in such a picture, where the total susceptibility is just a volume average of the susceptibilities of the two phases and thus *must* increase linearly in the mixed-phase region.

Recent electrochemical measurements [6] of the spin susceptibility in Na-doped polyacetylene have shown that its rapid increase occurs at a constant electrochemical potential, which was taken as evidence for a first-order transition. At the same time, Shacklette and Toth [30] showed that a mixed-phase regime occurs in Na-doped polyacetylene, in that the electrochemical potential is constant over concentrations between 0.01 and 0.06. The voltage in the mixed-phase region is the same as the voltage at which the susceptibility increases. If we assume that results for donor-doped (e.g., Na) and acceptor-doped (e.g., ClO_4) samples safely may be compared, then we note that there must be *three* distinct phases: (1) nearly undoped, semiconducting polyacetylene; (2) a highly-conducting, low susceptibility phase, corresponding to small ClO_4 clusters between $(\text{CH})_x$ layers [23]; and (3) a highly-conducting, high susceptibility phase, corresponding to a three-dimensionally-ordered intercalated structure [23]. There would seem to be little difference in the optical spectra of these latter two phases. Both show strong vibrational features in the infrared and an electronic absorption below the primary interband transition. Only the primary interband transition is absent in the third phase.

The first-order transition in the susceptibility led Kivelson and Heeger [31] to propose that heavily-doped polyacetylene is a polaronic metal. According to this model, two polaronic subbands exist within the Peierls gap (which is unchanged in magnitude from undoped polyacetylene). One subband (the upper in the case of donor doping and the lower for acceptor doping) is half filled, allowing for high d.c. and far-infrared conductivity and a large Pauli susceptibility, as observed. The model maybe consistent with the observation of doping-induced vibrational features in the infrared spectrum, although a recent calculation by Hicks *et al.* [32] finds a very small oscillator strength in these modes for the polaron lattice case. Our observation of a rather high oscillator strength would then be inconsistent with the presence of a polaron lattice. Further, it is not clear that the polaronic metal model could explain the presence of only a single strong electronic absorption in the data for Figs. 2 and 3. The optical absorption spectrum is not addressed in [31]. Fesser, Bishop and Campbell [33] have described in detail the absorption by low concentrations of polarons. They find that there are three transitions at frequencies below the primary interband transition: (1) from the lower polaron subband to the upper one; (2) from the valence band to the lower polaron subband (acceptor doping), or, from the upper one to the conduction band (donor doping); and (3) from the valence band to the upper polaron subband (acceptors), or, from the lower one to the conduction band (donors). Using parameters appropriate to polyacetylene they find that the third of these transitions is very weak but that the first and second have large, nearly equal strengths. Assuming a 1.4 eV Peierls gap, these absorptions would occur near 0.25 and 1.0 eV. Note that our data for heavily doped polyacetylene show only a single peak and thus appear to be inconsistent with the presence of polarons. Finally, the primary interband transition could exist (with reduced oscillator strength) in the polaron case; the symmetry which eliminates it from the soliton lattice [27] absorption does not hold for a polaron lattice. This transition is absent from our heavily-doped samples.

7. CONCLUSIONS

In summary, heavily-doped $(\text{CH})_x$ is not a simple metal as generally has been believed. There is no closed-gap, uniform-bond state; instead, the bond length distortion of $[\text{CH}(\text{ClO}_4)_y]_x$ becomes uniformly incommensurate when $y > 0.045$. The signature of this transition is a rise of the density-of-states at the Fermi surface (the gapless state-induced by disorder) and a disappearance of the $2\Delta_c$ interband transition. Although some details will differ, this picture should apply to

(CH)_x doped with other donors and acceptors as well as to other polymeric conductors.

Acknowledgements — This research was supported by the National Science Foundation, Solid State Chemistry, through DMR-8218021 and DMR-8416511.

REFERENCES

1. C.K. Chiang, C.R. Fincher, Y.W. Park, A.J. Heeger, H. Shirakawa, E.J. Louis, S.C. Gau & A.G. MacDiarmid, *Phys. Rev. Lett.* **39**, 1098 (1977).
2. K. Seeger, W.D. Gill, T.C. Clarke & G.B. Street, *Solid State Commun.* **28**, 873 (1978); K. Mortensen, M.L.W. Thewalt, Y. Tomkiewicz, T.C. Clarke & G.B. Street, *Phys. Rev. Lett.* **45**, 490 (1980); E.K. Sichel, M.F. Rubner, J. Georger, Jr., C.G. Papefthymiou, S. Ofer & R.B. Frankel, *Phys. Rev.* **B28**, 6589 (1983); S. Roth, *Physica* **127B**, 151 (1984).
3. Y. Tomkiewicz, T.D. Schultz, H.B. Broom, A.R. Taranko, T.C. Clarke & G.B. Street, *Phys. Rev.* **B24**, 4348 (1981).
4. S. Ikehata, J. Kaufer, T. Woerner, A. Pron, M.A. Druy, A. Sivak, A.J. Heeger & A.G. MacDiarmid, *Phys. Rev. Lett.* **45**, 1123 (1980); A.J. Epstein, H. Rommelmann, M.A. Druy, A.J. Heeger & A.G. MacDiarmid, *Solid State Commun.* **38**, 683 (1981).
5. T.-C. Chung, F. Moraes, J.D. Flood & A.J. Heeger, *Phys. Rev.* **B29**, 2341 (1984).
6. J. Chen, T.-C. Chung, F. Moraes & A.J. Heeger, *Solid State Commun.* **53**, 757 (1985); F. Moraes, J. Chen, T.-C. Chung & A.J. Heeger, *Syn. Metals* **11**, 271 (1985).
7. D. Moses, A. Dennenstein, A. Pron, A.J. Heeger & A.G. MacDiarmid, *Solid State Commun.* **36**, 219 (1980).
8. C.R. Fincher, Jr., M. Ozaki, M. Tanaka, D. Peebles, L. Lauchlan, A.J. Heeger & A.G. MacDiarmid, *Phys. Rev.* **B20**, 1589 (1979); M. Tanaka, A. Watanabe & J. Tanaka, *Bull. Chem. Soc. Japan* **53**, 3430 (1980); A. Feldblum, J.H. Kaufman, S. Etemad, A.J. Heeger, T.-C. Chung & A.G. MacDiarmid, *Phys. Rev.* **B26**, 815 (1982).
9. J.J. Ritsko, E.J. Mele, A.J. Heeger, A.G. MacDiarmid & M. Ozaki, *Phys. Rev. Lett.* **44**, 1351 (1980); J.J. Ritsko, *Phys. Rev. Lett.* **46**, 849 (1981).
10. Preliminary results were reported in X.Q. Yang, D.B. Tanner, A. Feldblum, H.W. Gibson, M.J. Rice & A.J. Epstein, *Mol. Cryst. Liq. Cryst.* **117**, 267 (1985).
11. H.G. Schuster, *Solid State Commun.* **14**, 127 (1974).
12. M.J. Rice, S. Strassler & W. Schneider, *Lect. Notes in Physics* **34**, 282 (1975).
13. M.J. Rice & E.J. Mele, *Chemica Scripta* **17**, 121 (1981); E.J. Mele & M.J. Rice, *Phys. Rev.* **B23**, 5397 (1981).
14. H. Shirakawa & S. Ikeda, *Polym. J.* **2**, 3 (1971).
15. M.J. Rice, *Phys. Lett.* **A71**, 152 (1979); W.P. Su, J.R. Schrieffer & A.J. Heeger, *Phys. Rev. Lett.* **42**, 1698 (1979); *Phys. Rev.* **B22**, 2099 (1981).
16. A.J. Epstein, H. Rommelmann, R. Bigelow, H.W. Gibson, D.M. Hoffman & D.B. Tanner, *Phys. Rev. Lett.* **50**, 1866 (1983); A.J. Epstein, R.W. Bigelow, H. Rommelmann, H.W. Gibson, R.J. Weagley, A. Feldblum, D.B. Tanner, J.P. Pouget, J.C. Pouxviel, R. Comes, P. Robin & S. Kivelson, *Mol. Cryst. Liq. Cryst.* **117**, 147 (1985).
17. N. Suzuki, M. Ozaki, S. Etemad, A.J. Heeger & A.G. MacDiarmid, *Phys. Rev. Lett.* **45**, 1209 (1980).
18. C.R. Fincher, Jr., M. Ozaki, A.J. Heeger & A.G. MacDiarmid, *Phys. Rev.* **B19**, 4140 (1979).
19. E.J. Mele & M.J. Rice, *Phys. Rev. Lett.* **45**, 926 (1980).
20. B. Horowitz, *Phys. Rev. Lett.* **47**, 1491 (1981); *Solid State Commun.* **41**, 593 (1982).
21. Z. Vardeny, E. Ehrenfreund, O. Brafman & B. Horowitz, *Phys. Rev. Lett.* **51**, 2326 (1983).
22. J.F. Rabolt, T.C. Clarke & G.B. Street, *J. Chem. Phys.* **71**, 4614 (1979); C. Benoit, O. Bernard, M. Palpacuer, M. Rolland & M.J.M. Abadie, *J. de Physique* **44**, 1307 (1983).
23. J.P. Pouget, J.C. Oouxviel, P. Robin, R. Comes, D. Begin, D. Billaud, A. Feldblum, H.W. Gibson & A.J. Epstein, *Mol. Cryst. Liq. Cryst.* **117**, 75 (1985).
24. K. Maki in *Superconductivity*, Vol 2, p. 1035, (Edited by R.D. Parks), Marcel Dekker, New York, (1969).
25. M.J. Rice, *Phys. Rev. Lett.* **37**, 36 (1976).
26. M. Jestin, M. Kabbaj, J.P. Albert & C. Jouanin, *J. de Physique* **44**, Colloq. **C3**, 499 (1983).
27. S. Jeyadev & E.M. Conwell, *Phys. Rev.* **B33**, 2530 (1986).
28. M.J. Rice, unpublished.
29. Dionys Baeriswyl & Kazumi Maki, *Phys. Rev.* **B31**, 6633 (1985).
30. L.W. Shacklette & J.E. Toth, *Phys. Rev.* **B32**, 5892 (1985).
31. S. Kivelson & A.J. Heeger, *Phys. Rev. Lett.* **55**, 308 (1985).
32. J.C. Hicks, J. Tinka Gammel, H.Y. Choi & E.J. Mele, *Synth. Met.*, in press; preprint.
33. K. Fesser, A.R. Bishop & D.K. Campbell, *Phys. Rev.* **B27**, 4804 (1983).